UNCLASSIFIED

CRDV RAPPORT 4060/77
DOSSIER 36348-001
JANVIER 1977

3

CRDV REPORT 4060/77
FILE 36348-001
JANUARY 1977

OPTIMIZATION OF THE PRE-PUMPING NO/ClO_2 CHEMISTRY IN A PURELY CHEMICAL HCl LASER

K.D. Foster, D.R. Snelling

R.D. Suart and S.J. Arnold

Centre de Recherches pour la Défense
Defence Research Establishment
Valcartier, Québec

BUREAU - RECHERCHE ET DEVELOPPEMENT
MINISTERE DE LA DEFENSE NATIONALE
CANADA

NON CLASSIFIE

RESEARCH AND DEVELOPMENT BRANCH
DEPARTMENT OF NATIONAL DEFENCE
CANADA

CRDV R-4060/77
DOSSIER: 3634B-001

UNCLASSIFIED

DREV R-4060/77
FILE: 3634B-001

OPTIMIZATION OF THE PRE-PUMPING $NO/C\ell O_2$ CHEMISTRY IN A PURELY CHEMICAL HCℓ LASER

by

K.D. Foster, D.R. Snelling, R.D. Suart and S.J. Arnold

CENTRE DE RECHERCHES POUR LA DEFENSE

DEFENCE RESEARCH ESTABLISHMENT

VALCARTIER

Tel: (418) 844-4271

Québec, Canada

January/janvier 1977

RESUME

L'émission laser à 3.8 μm, provenant d'un laser au HCℓ purement chimique, a été utilisée pour recueillir des renseignements sur la chimie du prépompage par le système $NO/C\ell O_2$. La réaction entre les atomes de chlore produits chimiquement et l'iodure d'hydrogène fournit le mécanisme de pompage. Le laser a fonctionné efficacement selon trois différents modes cinétiques ou chimiques. Ces modes se différencient par la façon dont le chlore est introduit dans la cavité laser, soit directement sous forme d'atomes de chlore, de radicaux CℓO ou de molécules de $C\ell O_2$. La comparaison des résultats expérimentaux de ces deux derniers modes avec ceux d'une simulation par ordinateur sur la disparition du HCℓ permet d'expliquer les caractéristiques principales des relations entre la réaction de pompage et la chimie du prépompage. (NC)

ABSTRACT

The laser output at 3.8 μm from a purely chemical HCℓ laser was used to obtain information about the pre-pumping chemistry of the $NO/C\ell O_2$ system. The reaction of chemically produced chlorine atoms with hydrogen iodide was the laser pumping reaction. Successful laser operation was confirmed using three different kinetic or chemical modes. These modes are distinguishable by whether the chlorine enters the optical (laser) region directly in the form of chlorine atoms, CℓO radicals or parent $C\ell O_2$ molecules. A comparison of experimental results for the latter two modes, using computer simulation results for the time evolution of HCℓ, showed that the main features of the coupling of the pumping reaction to the pre-pumping chemistry are understood. (U)

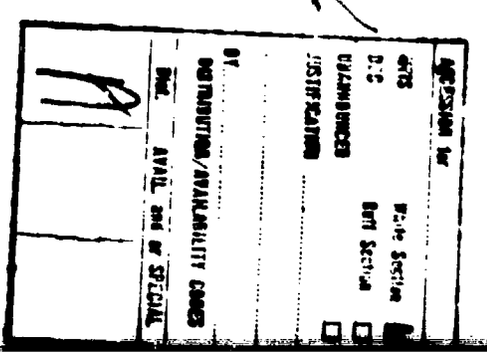

TABLE OF CONTENTS

1.0 INTRODUCTION

Lasers in which the population inversions are produced directly by elementary chemical reaction steps are termed 'chemical lasers'. This group can be further subdivided into: (a) purely chemical lasers, (b) electrically assisted chemical lasers, and (c) thermally pumped chemical lasers. In these three classes the lasing species, or its precursor, is produced: (a) by purely chemical means, (b) directly or indirectly by an electrical discharge, or (c) by thermal dissociation such as the combustor-type DF laser. To date, most chemical lasers have been based on vibration-rotation transitions and therefore produce radiation in the infrared region.

The hydrogen-halide chemical lasers have received the most attention. Of these, the HCℓ and DF chemical lasers have the particular advantage of producing laser emission in a wavelength region that is relatively free of absorption by atmospheric constituents. These systems operate in the 3.6 to 4.0 μm region.

For a reaction system to operate as a chemical laser, a substantial fraction of the elementary reaction exothermicity must appear as vibrational energy of the newly formed product molecule. Vibrationally excited HCℓ may be formed from the reaction:

$$Cℓ + HI \rightarrow HCℓ^{\dagger} + I \quad \Delta H = -32 \text{ kcal/mol}, \qquad (1)$$

in which some 70% of the reaction energy appears as vibration in the HCℓ molecule (Ref. 1). This system has been made to lase in both pulsed (Ref. 2) and CW (continuous wave) regimes (Refs. 3,4). The achievement of efficient CW laser action in this system, in which the atomic Cℓ was produced in an electrical discharge, has been demonstrated by Linevsky and Carabetta (Ref. 5).

A chemical mechanism for the formation of low concentrations of atomic chlorine by the reaction of NO with $C\ell O_2$ has been described elsewhere (Refs. 6 - 8). The mechanism involves the reaction of nitric oxide with chlorine dioxide producing atomic chlorine by the following reaction steps:

$$NO + C\ell O_2 \rightarrow NO_2 + C\ell O$$

$$k_2 = 3.3 \times 10^{-13} \text{ cm}^3 \text{ s}^{-1} \qquad (2)$$

$$NO + C\ell O \rightarrow NO_2 + C\ell$$

$$k_3 = 1.7 \times 10^{-11} \text{ cm}^3 \text{ s}^{-1} \qquad (3)$$

$$C\ell + C\ell O_2 \rightarrow 2C\ell O$$

$$k_4 = 5.9 \times 10^{-11} \text{ cm}^3 \text{ s}^{-1} \qquad (4)$$

The above rate coefficients were measured by Clyne (see Appendix A for references and a discussion of available rate data used in the computer simulations).

Purely chemical laser action based on this reaction sequence has recently been demonstrated at DREV. First, laser action was realized at 10.6 μm in a purely chemical $HC\ell/CO_2$ transfer laser employing longitudinal flow (Ref. 7). Subsequently, purely chemical laser action in $HC\ell$ in a transverse flow system was achieved (Ref. 8). Although the pre-pumping chemistry of the above reactions has been discussed in these previous studies, the essential features of the reaction sequence are described here. The overall effect of stripping the two oxygen atoms from the $C\ell O_2$ molecule by NO is achieved with a molar ratio of $NO/C\ell O_2$ of 2/1. The $C\ell$ atom and the $C\ell O$ radical act as chain carriers. As long as $C\ell O_2$ is present, atomic $C\ell$ produced in reaction (3) promotes chain branching in reaction (4). $C\ell O$ radicals build up initially because of reaction (4) and, to a lesser extent, reaction (2). Once all of the $C\ell O_2$ has been consumed, reaction (3) converts this accumulated $C\ell O$ into $C\ell$ atoms.

As noted previously, efficient chemical laser action in HCℓ employing NO and $C\ell O_2$ for atomic Cℓ production was achieved recently (Ref. 8). The well known Cℓ + HI reaction was the pumping reaction in the above study. A maximum of 4 W output power at 3.6 to 4.0 μm was observed, corresponding to a chemical efficiency of 6% based upon the total exothermicity of the pumping reaction. The maximum specific power relative to atomic chlorine was 288 J/gCℓ. Power levels of 2.0 to 2.5 W were typically observed. Laser emission originated from eight P-branch transitions of $HC\ell^{35}$ from the v=3→2, v=2→1 and v=1→0 vibrational bands. Typical J values ranged from J=5 to J=7.

The principal goal of the present study was to ascertain whether an HCℓ chemical laser relying upon NO and $C\ell O_2$ for Cℓ atom production could be operated under conditions that would allow scaling to supersonic velocities. Unlike the 'combuster' type supersonic HF and DF lasers, a supersonic device based upon the $NO/C\ell O_2$ system would not rely on thermal dissociation to produce atomic species in a high-temperature, high-pressure plenum. It would instead employ the non-equilibrium chemistry inherent in the $NO/C\ell O_2$ system to produce atomic Cℓ. However, the attainment of supersonic velocities necessarily requires the acceleration of a gas from a plenum at relatively high pressures, and it is believed that the non-equilibrium production of atomic Cℓ in a plenum would be plagued with high recombination losses of Cℓ. For this reason, the scaling of the HCℓ laser based upon $NO/C\ell O_2$ would appear to be severely limited if not precluded altogether. If, however, it were possible to delay production of the atomic Cℓ until the expanded (low-pressure) region was reached the high pressure in the plenum would be of little consequence.

The initial successful operation of a subsonic-flow HCℓ laser with *in situ* formation of Cℓ atoms was discussed previously (Ref. 8). The experiments reported herein are a continuation of this subsonic-flow

work in which an attempt is made to fully exploit the flexibility of the $NO/C\ell O_2$ system and thereby gain an insight into the conditions of pre-pumping chemistry which would be required for successful supersonic scaling of a chemical $HC\ell$ laser.

This work was conducted in mid-1975 under PCN 34B01 (formerly PCN 07C01, Project No. 97-01-39("Research on Chemically Excited Lasers".

2.0 EXPERIMENTAL

The experimental apparatus employed in the present experiments was described previously (Ref. 8). It consists of two main sections, a $C\ell O_2$ generator (Ref. 9, 10) and a transverse-flow laser. A schematic diagram of the arrangement appears in Fig. 1. The $C\ell O_2$ generator included columns containing $NaC\ell O_2$ in which conversion of the input $C\ell_2$ to $C\ell O_2$ occurred by the heterogeneous reaction:

$$C\ell_2 + 2NaC\ell O_2 \rightarrow 2NaC\ell + 2C\ell O_2 \qquad (5)$$

Measures taken for the safe handling of $C\ell O_2$ have been described previously (Refs. 7,8 & 10). The transverse flow laser was essentially the same as that described previously except for the following minor changes. The interior metal surfaces were covered with 1/16-in-thick teflon sheets. Moreover, for most experiments, an additional injector row was added 2 cm upstream from the row that was in line with the window section. The modified injector configuration therefore consisted of three injector rows extending across the 14-cm channel, with the last two rows located 10 cm and 12 cm downstream of the first row.

The optical cavity consisted of a 4-m-radius-of-curvature 'total' reflector of the protected metal type and a partially reflective decoupling flat having a nominal transmission of 4% at 3.85 μm.

Laser power measurements were performed with a Coherent Radiation power meter. Gas flows were monitored with Hastings-Raydist linear mass flow meters.

Typically, the experiments described herein were conducted under the following approximate flow conditions:

Helium (through $NaC\ell O_2$ columns)	12 mmol s^{-1}
$C\ell_2$ (through $NaC\ell O_2$ columns)	0.25 mmol s^{-1}
Auxiliary He	45 mmol s^{-1}
NO total	1-3 mmol s^{-1}
HI	0.5 mmol s^{-1}

Total Pressure 3-4 torr

Average Linear Velocity ~220 m s^{-1}

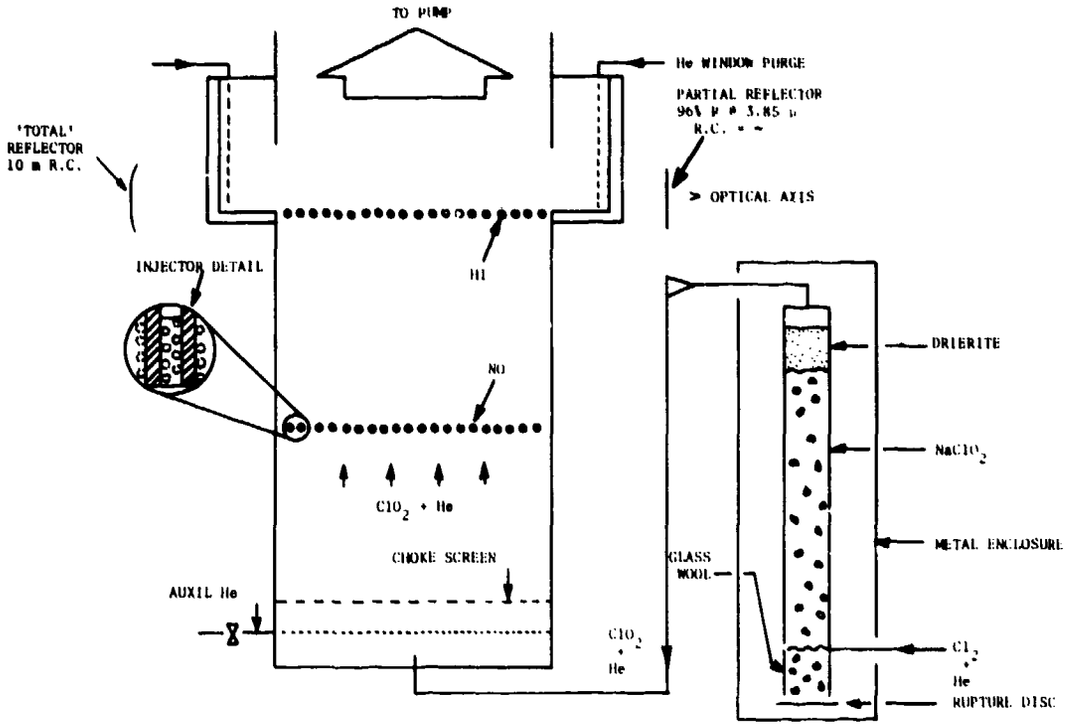

FIGURE 1 - Diagram of the Apparatus

3.0 COMPUTER SIMULATION OF CHEMICAL KINETICS

A computer simulation of the chemical processes taking place in the laser cavity has been carried out for a variety of experimental conditions. A complete list of the chemical reactions considered together with the relevant rate constants is given in Appendix A. The computer program used to calculate the time evolution of the reacting species is 'Dolphin', a general program for the treatment of chemical rate equations (Ref. 11).

A complete description of these calculations will be given in a later publication (Ref. 12)); hence, only an outline of the method will be included here. The following assumptions were made in the computations: mixing was instantaneous and temperature in the gas stream was constant at 300 K. However, mixing is not instantaneous and may extend into the optical region. The assumption of instantaneous mixing is nevertheless employed in the computer simulations since kinetic trends and processes, rather than fluid dynamic ones, are of primary interest here. In a real experimental apparatus, the effect of a finite mixing time would be one of limiting the rates of certain processes having large rate coefficients. The reaction rate would therefore be 'diffusion controlled'. (Although this effect reduces the accuracy of the computer-generated specie concentrations at early reaction times, it should not alter conclusions about kinetic trends.) The second assumption was dictated principally by the fact that the majority of the kinetic rate data required have been determined for 300 K only. Thermochemical considerations suggest that the temperature in the laser region is below 400 K at the optimum diluent flow rate.

The HCℓ formation has been taken as a 'figure of merit' rather than the gain on each of the possible vibrational-rotational transitions. In taking total HCℓ as a figure of merit we have neglected vibrational-

vibrational deactivation of excited HCℓ. This process, as well as other deactivation processes, will lead to a scrambling of the initial population distribution and a consequent loss of gain and, hence, extractable laser power. However, since no reliable model of the deactivation process is available at this time we have chosen to model the HCℓ formation reactions only. Consequently, a detailed knowledge of the time dependence of the temperature and of the effect of relaxation processes on the individual level populations was not required.

4.0 RESULTS AND DISCUSSION

4.1 Operation in Three Chemical Modes

An inherent advantage of the chemical HCℓ laser based on the reaction of NO with $C\ell O_2$ lies in its flexibility. The possibility of operating the laser in different chemical modes was mentioned previously (Ref. 8). These may be categorized and described as:

MODE I - Chemical Cℓ production followed by HI addition. The first HCℓ paper (Ref. 8) dealt primarily with this mode that consists of an upstream injection of NO sufficient to convert all of the $C\ell O_2$ to atomic Cℓ. Hydrogen iodide is then added at a downstream location to produce vibrationally excited HCℓ. This mode of operation is directly analogous to the electrically assisted HCℓ laser (Ref. 3-5), in which atomic Cℓ is produced electrically and subsequently allowed to react with HI.

MODE II - Preconversion of all or part of the initial $C\ell O_2$ to CℓO radicals followed by NO and HI addition, the 'Split NO Method'. Preliminary results relying on this method were reported previously (Ref. 8). Operation in this mode allows storage of the atomic Cℓ in the form of the CℓO radical

until needed. This is accomplished with a reduced NO flow through the upstream injectors. The requisite Cℓ for the pumping reaction is later released with a final addition of NO and HI which initiates the reaction steps:

$$NO + C\ell O \rightarrow NO_2 + C\ell \qquad (3)$$

$$C\ell + HI \rightarrow HC\ell^{\dagger} + I \qquad (1)$$

MODE III - Single-Step Chemistry Mode: If the logic upon which the Split NO Flow Method is based is extended, then the possibility of a third chemical mode arises. This mode of operation would allow for the occurrence of all requisite chemical reactions and the pumping step after one simple addition of NO. The Cℓ would thereby be stored in its most stable useable form, namely, as the parent $C\ell O_2$ molecule. In this configuration the mainstream may consist of $C\ell O_2$ and HI with a suitable diluent, and reaction would commence upon addition of NO. It was anticipated that the chain nature of the reaction sequence would put an upper limit on the permissible concentration of HI since HI would remove chain carriers. As will be noted later, however, experiments showed that with an excess of NO, the laser did not rely on a chain mechanism, and no such upper limit on the HI concentration was apparent.

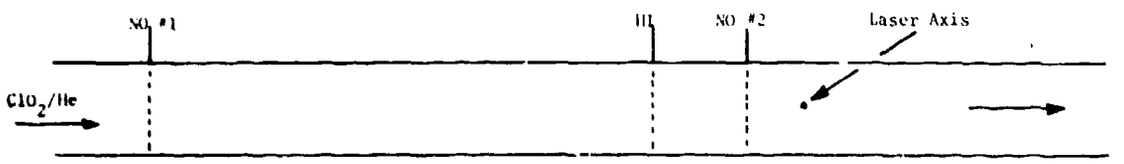

FIGURE 2 - Injector Configuration

The present paper deals primarily with MODE II and MODE III. The injector configuration that was employed for these experiments is shown in Fig. 2. In principle, one downstream injector row for the NO #2 and HI could be used. However, experiments indicated that when the NO #2 and HI were previously mixed in a high-pressure region (i.e., in either the HI or NO #2 line), molecular iodine formation resulted which clogged the injector holes. For this reason, an additional injector row was inserted 2 cm upstream of the final injector so that NO #2 and HI were added separately, yet as close together as the flow geometry of the apparatus would allow. It has been shown previously that there is sufficient time (typically 500 μs) between the NO #1 and downstream injectors to allow the chain chemistry to go to completion (Ref. 8).

4.2 The Transition from MODE II to MODE III: Split NO Addition Experiments

The dependence of HCℓ laser power as a function of the fraction of total NO_T entering through the upstream injector row at four different total NO_T flow rates is illustrated in Fig. 3. For each total NO flow, the power was measured at distances of 1 cm and 1.8 cm downstream of the NO #2 injector. These two positions on the optical axis correspond to flow times of ∿50 and ∿85 μs from the final injector. The HI and $C\ell O_2$ flow rates for these experiments were 1000 SCCM. The $C\ell O_2$ flow rate is approximate since it was based on the $C\ell O_2$ input to the columns and an assumed value of 85% conversion of the Cℓ to $C\ell O_2$ (each molecule of $C\ell_2$ can produce two molecules of $C\ell O_2$) in the $NaC\ell O_2$ columns. Quantitative measurements of the output of $C\ell O_2$ from the columns indicate a typical conversion of ∿80% for the experimental conditions used here.

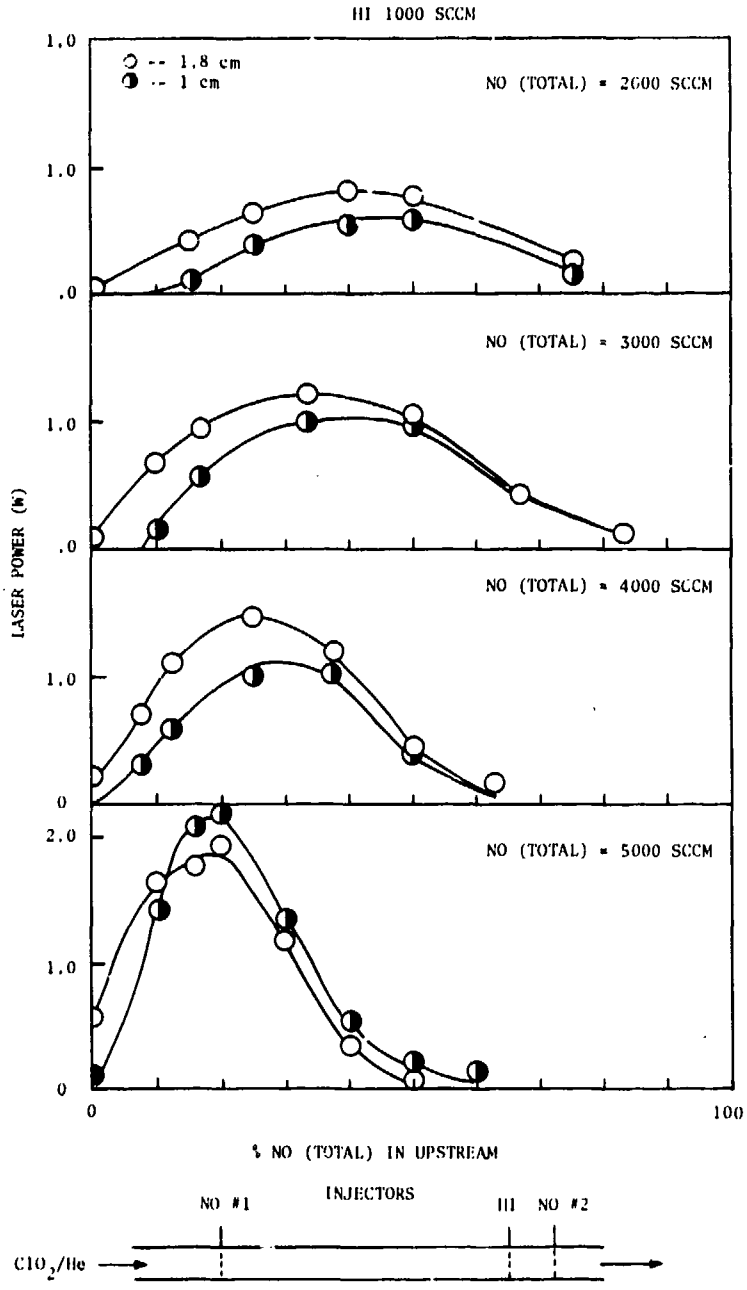

FIGURE 3 - Dependence of the Laser Power on the "Percentage NO (TOTAL) through the Upstream Injectors" for different total NO flows. The open circles (O) correspond to results with the laser axis 1.8 cm from the NO #2 injector. The half-open circles apply to results with the laser axis 1 cm from NO #2.

For total NO, NO_T, flow values of 2000, 3000, 4000 and 5000 SCCM, the laser power reached a maximum at 45%, 35%, 30% and 20% respectively of total NO_T through the upstream injectors, corresponding to absolute flow rates of NO through the upstream injectors of 900, 1060, 1200 and 1000 SCCM. These flows were approximately equivalent to the input $C\ell O_2$ flow rate, which corresponded to the complete conversion of $C\ell O_2$ to $C\ell O$ radicals before reaching the HI and NO #2 inlets. One would expect the output power to increase to a plateau value as the percent NO flowing in the upstream injector was increased. In fact, the power attained a certain value but then began to decrease. This was a result of the geometrical constraints of the laser that made the point of HI injection slightly upstream of, rather than coincident with, the NO #2 injector. As the fraction of NO through the upstream injectors was increased, an NO flow through the upstream injectors was reached that corresponded to complete conversion to $C\ell O$ radicals. Above this percentage of NO, the $C\ell O$ radicals were converted to atomic $C\ell$, which reacted with HI to form $HC\ell$ at the HI injector. This $HC\ell$ was wasted, however, since it was largely deactivated before reaching the optical axis located 3 or 4 cm downstream of the HI injectors. For this reason, the laser power decreased as the point of 100% NO_T through the upstream injectors was approached.

A number of other features in Fig. 3 should also be pointed out. It appears that the distance at which maximum gain occurred moved upstream as the total NO (NO_T) was increased to a point where the power was higher at 1 cm than at 1.8 cm for a flow of NO_T of 5000 SCCM. This NO flow is 2.5 times the stoichiometric requirement of NO. For lower total NO_T flows, the highest power was observed at the downstream optical axis location.

Figure 4 shows modelling results for the time dependence of formation of $HC\ell$ at various extents of preconversion of $C\ell O_2$ into $C\ell O$ radicals. These curves correspond to initial concentration ratios

of $C\ell O_2$:(total) NO_T:HI of 1:5:1. The $C\ell O_2$ concentration (1×10^{15} cm^{-3}) was approximately equal to that used in the laser. The bottom curve corresponds to no preconversion, or MODE III operation, while the top curve corresponds to complete preconversion, of MODE II operation. In comparison, it should be noted that the laser axis is located in a region for which the flow time from the injection is ∿50 to ∿85 μs. At early reaction times the beneficial effect of even slight extents of preconversion in optimising the rapid formation of HCℓ is apparent. This appears to be borne out by experimental curves in Fig. 3.

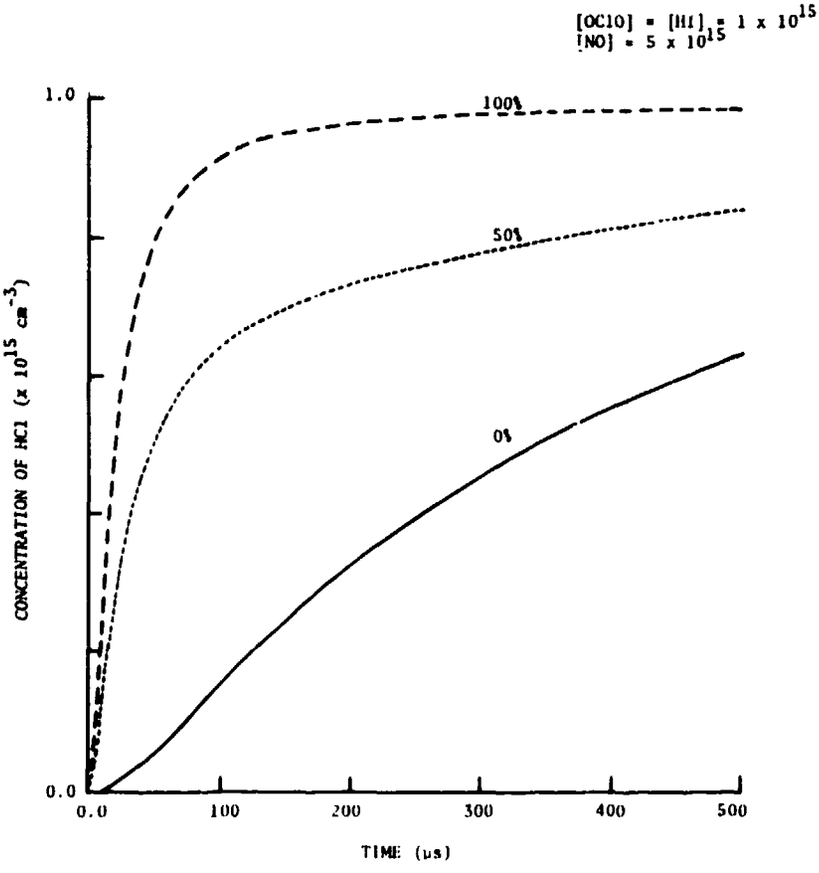

FIGURE 4 - Total HCℓ formation as a function of the extent of preconversion of $C\ell O_2$ to ClO

4.3 Chemical MODE III

The HCℓ power corresponding to zero percent NO through the upstream injectors in Fig. 3 corresponds to operation in the chemical MODE III described previously. In this mode, in which all of the requisite chemistry commences at the final NO injection point, the power is highest under conditions of high total NO_T flow and at the downstream optical axis location. A subsequent experiment under conditions of somewhat higher total NO_T flow, in which the NO flow was beyond the range of the 5000 SCCM flow meter, resulted in an output power of 1.0 W being observed in this mode, i.e., MODE III.

4.3.1 Effect of HI Flow Rate on HCℓ Laser Power

The dependence of the laser output power on the HI flow rate was examined for MODE III operation. The total flow of NO_T, 4100 SCCM, was directed entirely through the downstream injector row. This dependence is shown in Fig. 5. The laser power increases rapidly with increasing HI and reaches a maximum value of 0.3 W at an HI flow of about 1000 SCCM. Further addition of HI leads to only a slight reduction in power. This result was somewhat surprising since it was believed that the laser power would drop precipitously at high HI flows due to overloading of the chemical chain. In other words, if too many Cℓ atoms were withdrawn from the chain cycle by reaction with HI, then it was expected that the all important branching reaction:

$$Cℓ + ClO_2 \rightarrow 2ClO \qquad (4)$$

would be quenched. A possible explanation for the absence of this rapid decrease of laser power with HI flow at high HI flows was found when the kinetics corresponding to MODE III operation were modelled.

The calculated time dependence of HCℓ formation under MODE III conditions at various HI initial concentrations is shown in Fig. 6. It will be recalled that this corresponds to single step NO addition, in

which all of the chemistry, including laser pumping, is promoted in one step. The initial $C\ell O_2$ and NO concentrations, 10^{15} and 4×10^{15} cm^{-3} respectively, are similar to the experimental conditions which prevailed for Fig. 5. It will be noted that HCℓ formation is virtually independent of HI at reaction times less than 150 μs. At high HI concentrations not enough Cℓ is allowed to react with $C\ell O_2$ to make the branching reaction $C\ell + C\ell O_2 \rightarrow 2C\ell O$ the dominant source of CℓO radicals. Because of the higher NO concentration, however, the reaction takes on a non-chain character involving:

$$NO + C\ell O_2 \rightarrow NO_2 + C\ell O \qquad (2)$$

$$NO + C\ell O \rightarrow NO_2 + C\ell \qquad (3)$$

$$C\ell + HI \rightarrow HC\ell^{\dagger} + I \qquad (1)$$

with the CℓO radicals provided by reaction (2).

Because of the absence of the branching step, the overall reaction time is greatly increased. The build-up of HCℓ is then far from complete at ∿80 - 100 μs, which is the approximate reaction time 'seen' on the laser axis. The observed low power levels and insensitivity to HI at the high HI flow shown in Fig. 3 would therefore be consistent with this kinetic model.

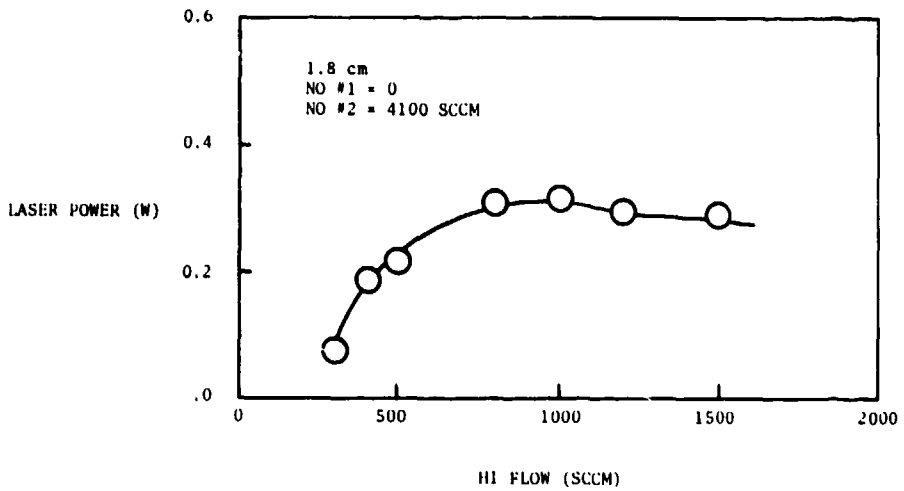

FIGURE 5 - HCℓ Laser Power vs HI flow. Laser axis is 1.8 cm from NO #2 Flows correspond to Kinetic Mode III with NO #1 = 0 and NO #2 = 4100 SCCM.

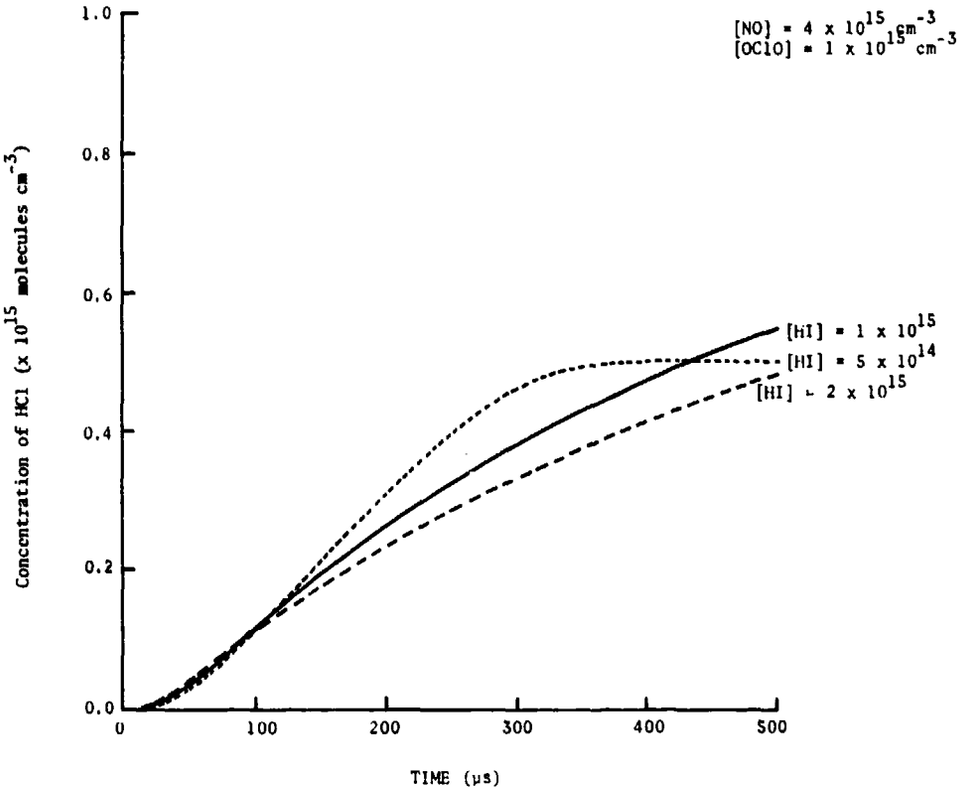

FIGURE 6 - Effect of HI concentration on HCℓ formation for Chemical (Kinetic) MODE III

4.3.2 The Importance of Initial Step: NO + $C\ell O_2$

Consider the pre-pumping reaction sequence for the NO + $C\ell O_2$ system:

$$NO + C\ell O_2 \rightarrow NO_2 + C\ell O \quad (2)$$

$$NO + C\ell O \rightarrow NO_2 + C\ell \quad (3)$$

$$C\ell + C\ell O_2 \rightarrow 2C\ell O \quad (4)$$

As discussed above, for conditions of large excess NO flow and small extents of preconversion, reaction (2) should become more important relative to reaction (4). Under these conditions, the existence or not of an activation energy for reaction (2) is important

(See Ref. 2 for a discussion of the possible temperature dependence of these reactions). Figure 7 shows the effect of a two-fold increase in the rate coefficient for reaction (2) on the HCℓ formation rate. A simple computation assuming an Arrhenius type temperature dependence of the rate coefficient reveals that if reaction (2) had an activation energy of ∿4 kcal/mol, the rate coefficient at 335 K would be twice its value at 300 K. Such temperature variations are possible in the present HCℓ laser. The time required for maximum HCℓ formation is markedly reduced if the rate constant for the NO + $C\ell O_2$ → NO_2 + CℓO reaction step is increased twofold. The laser power may therefore be sensitive to temperature for kinetic reasons as well as for optical gain reasons.

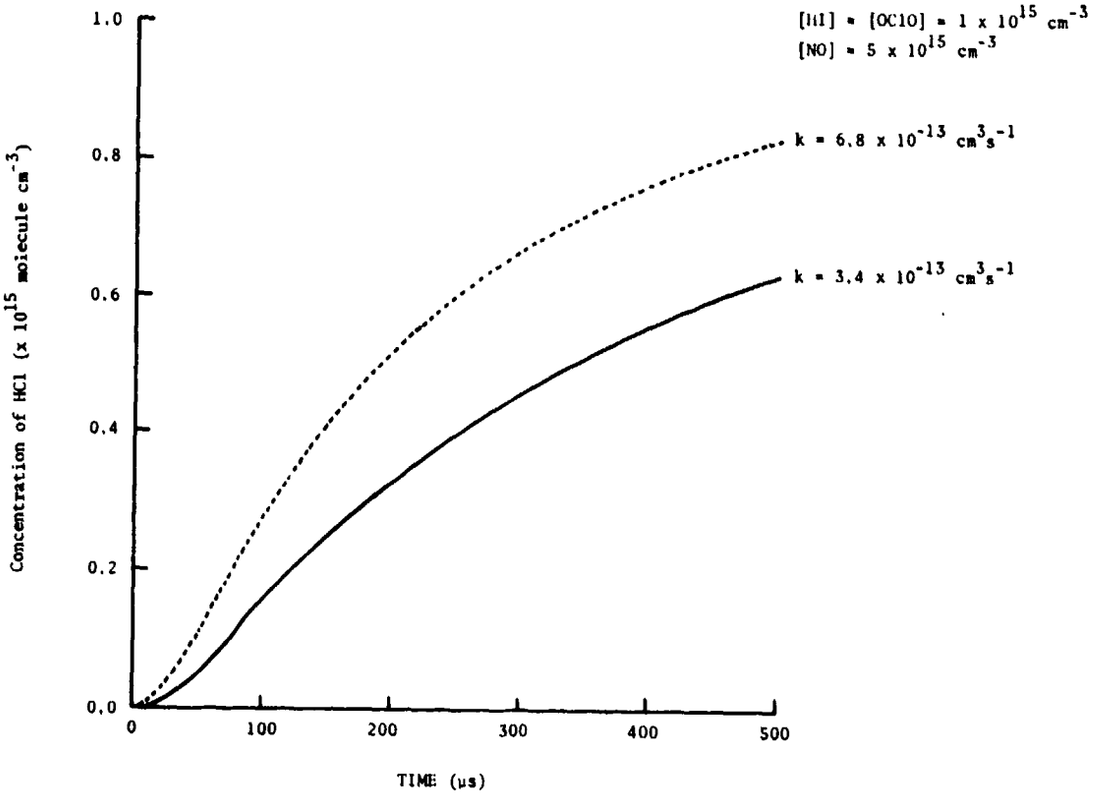

FIGURE 7 - Effect of Changing the Rate Coefficient for NO + $C\ell O_2$ → NO_2 + CℓO on the total HCℓ formation

The dependence of the laser power on the diluent helium flow was examined for MODE III operation and is shown in Fig. 8. Also shown as a solid curve, at the right-hand side ordinate, is a calculated maximum adiabatic temperature for each diluent helium flow. Fluid dynamic factors such as the momentum flux ratio between the free stream and the injected gases, as well as the temperature dependence of relevant molecular diffusion coefficients, will no doubt play a role in affecting the shape of the curve in Fig. 8. However, the observed maximum in Fig. 8 may also reflect the existence of an activation energy in reaction (2). An excess of He may reduce the pumping rate by lowering the ambient temperature.

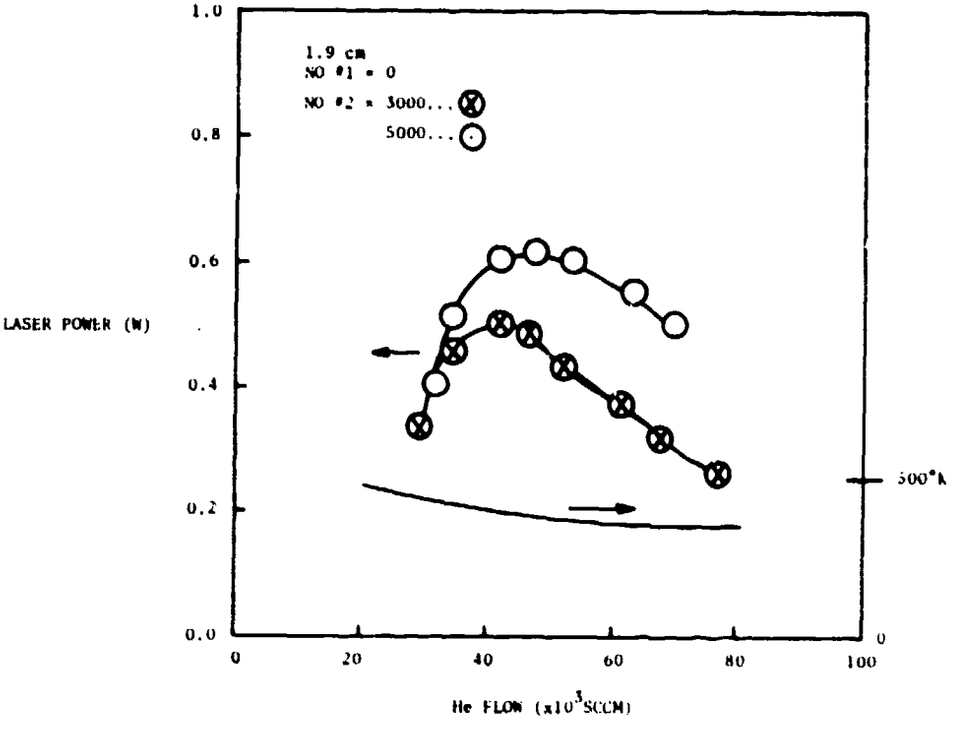

FIGURE 8 - Dependence of HCℓ Laser Power on diluent Helium Flow. Chemical MODE III

The results which have been discussed above, particularly the model generated curves of Fig. 5, show that even with large excesses of NO and complete preconversion of the $C\ell O_2$ to $C\ell O$ radicals, approximately 100 μs are required before the formation of $HC\ell$ is essentially complete. For scaling reasons, it would be desirable to increase the rate of $HC\ell$ formation. In principle this may be accomplished by operating under conditions in which <u>both</u> $C\ell O_2$ and NO are substantially in excess of the HI initial concentration. Unfortunately, the capacity of the $C\ell O_2$ generator used for the present experiments was not sufficient to allow large excesses of $C\ell O_2$ and, therefore, an experimental confirmation of the forementioned statement. The time dependence of the formation of $HC\ell$ as predicted by the model, under conditions of a threefold excess of $C\ell O_2$ over HI for various NO flows, is shown in Fig. 9. These curves demonstrate that in the single-step addition regime, in which <u>none of the $C\ell O_2$</u> is preconverted to $C\ell O$ (i.e., MODE III), it is possible to effect complete formation of $HC\ell$ in about 80 μs at the HI concentration levels that prevail in the present experiment. The modelling calculations show that operation under conditions of excess $C\ell O_2$ <u>and</u> NO would ensure that sufficient $C\ell$ chain carriers are kept in the chain cycle to allow the chain-branching step $C\ell + C\ell O_2 \rightarrow 2C\ell O$ to proceed parallel to the $HC\ell$ forming reaction $C\ell + HI \rightarrow HC\ell^{\dagger} + I$.

As mentioned previously, the experiments described here were carried out for conditions corresponding to chemical MODES II and III. The power levels that were obtained did not exceed or even equal those observed previously for MODE I operation.

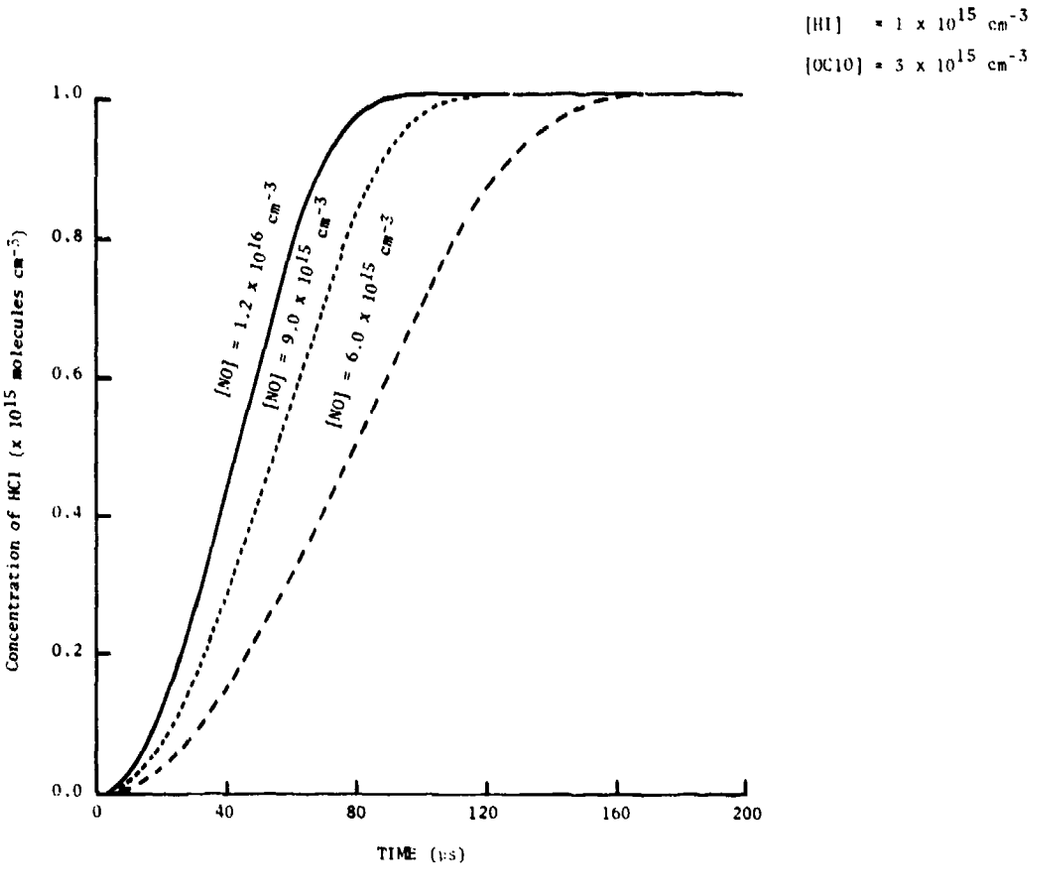

FIGURE 9 - HCℓ formation for various NO flows. MODE III ($C\ell O_2$) ≡ 3 x 10^{15} cm^{-3} (HI) ≡ 10^{15} cm^{-3}

4.4 Relaxation Processes

The relaxation processes for $HC\ell_v$ have been discussed in detail in Ref. 12. At present, insufficient rate data exists to adequately describe the V-V exchange processes of HCℓ with HCℓ or HCℓ with HI. Adequate rate data exists only for the relaxation (V→TR) of $HC\ell_v$ by Cℓ, $C\ell_2$, NO and HCℓ (v=0). The deactivation of $HC\ell_v$

$$HC\ell_v + X \rightarrow HN\ell_{v-1} + X$$

by each of these species was considered separately in order to determine which of these collision processes was of prime importance. Deactivation of $HC\ell_v$ by the species NO_2, I, I_2, O_2, HI (v=0) and $NOC\ell$, all of which may be present in appreciable concentrations at various times in the evolution of the lasing mixture, could not be considered due to the lack of rate data.

If one considers the number of diatomic and polyatomic species present in the $NO/C\ell O_2/HI$ system, one may reasonably inquire about possible ways in which $HC\ell$ may lose its vibrational energy to various collision partners. Specifically, is it possible to account for the lower powers observed for MODES II and III operations than for MODE I operation by differences in the extent of relaxation for the three modes? Since the vibrationally excited $HC\ell$, initial HI and product NO_2 concentrations were about the same for all three modes of operation, self-relaxation by $HC\ell$ and V-V transfer from $HC\ell$ to HI or to NO_2 cannot account for the observed differences in power levels.

Other possible processes which may deplete the $HC\ell_v$ concentration are:

$$HC\ell_v + C\ell \rightarrow HC\ell_{v-1} + C\ell \qquad (6)$$

$$HC\ell_v + NO \rightarrow HC\ell_{v-1} + NO(v=1) \qquad (7)$$

Collisions between $HC\ell_v$ and $C\ell O_2$ and $C\ell O$ may also deactivate $HC\ell_v$. Process (6) is known to be rapid (Ref. 13). Indeed, the speed of this process was one of the reasons why it was believed that operation in MODES II and III might give even higher output powers than that in MODE I, since the ambient $C\ell$ atom concentration should be much lower in MODES II and III operations. Since power levels are lower in MODES II and III operations, another process, or processes, apparently more than offsets the advantage of low $C\ell$ concentration. Generally, MODES II and III are characterized by higher ambient $C\ell O$, $C\ell O_2$ and NO concent-

rations than is MODE I. In MODE II operation, in which the $C\ell O_2$ is preconverted to $C\ell O$ radicals, intimate contact is possible between $HC\ell^\dagger$ and $C\ell O$. In MODE III, the parent $C\ell O_2$ molecule may undergo many collisions with $HC\ell^\dagger$. Little is known about the transfer of vibrational quanta from $HC\ell^\dagger$ to $C\ell O_2$.

In most of the MODE II and MODE III experiments described in the present paper the optimum NO concentration substantially exceeded the levels that prevailed in MODE I operation. The possible depletion of $HC\ell^\dagger$ by V-V transfer to NO must therefore be considered. The v=1→0 vibrational level spacing is 2886 cm^{-1} for $HC\ell$ and 1876 cm^{-1} for NO. The probability of a transfer from $HC\ell_{v-1}$ to NO has been measured by Zittel and Moore (Ref. 14) as 4.2×10^{-4} despite the large energy discrepancy of 1010 cm^{-1}. The corresponding energy discrepancy for $HC\ell(v=2\rightarrow1)/NO$ is 906 cm^{-1} and for $HC\ell(v=3\rightarrow2)/NO$ it is 803 cm^{-1}. An approximate correlation between the transfer probabilities and the energy defect (Ref. 14) was employed to estimate the probabilities for transfer of a vibrational quantum from $HC\ell_{v=2}$ to NO and from $HC\ell_{v=3}$ to NO. For this calculation, a reduced transfer probability $\frac{P(v\rightarrow v-1)}{v}$ was determined from the energy defect. With the experimental value of (0.42×10^{-13}) for v=1, values for v=2, 3 and 4 were calculated to be (0.65×10^{-3}), $(1.\ \times 10^{-3})$ and (1.7×10^{-3}) respectively. Some loss of $HC\ell$ quanta is expected at the highest NO concentration used in the present experiments (i.e., [NO] $\sim 5 \times 10^{15}$ cm^{-3}). Based upon the above probabilities, within the time of interest ($\sim$200 μs), loss of $HC\ell_v$ is expected particularly from $HC\ell_{v=3,4}$.

Figure 10 gives a plot of $HC\ell$ laser power vs NO input. The experiment was performed using only two injector rows. All of the NO was added through the upstream rows and the HI was added downstream near the optical region. This experiment therefore corresponded to operation in chemical MODE I. The curve was extrapolated to the highest NO level prevalent in MODE II and MODE III operations. The

extrapolated output power at this NO input rate was only about one half the maximum observed power. Under these experimental conditions, the total pressure and NO concentration were too low to account for this power decrease through NO catalyzed recombination losses of Cℓ (Ref. 15). This result would suggest that the increased importance of V-V $HC\ell^{\dagger}$ - NO transfer in MODES II and III operations relative to MODE I operation may account for the reduced laser output in MODES II and III.

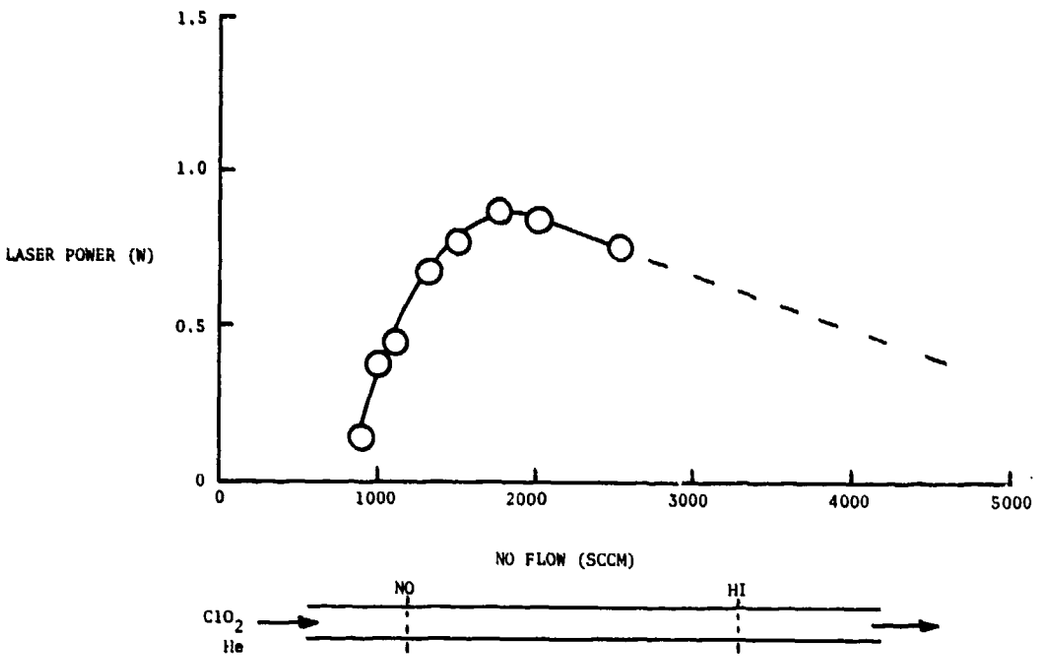

FIGURE 10 - HCℓ Laser Power vs NO Flow Rate MODE I.

5.0 CONCLUSIONS

The regime that was studied previously (Ref. 8), and referred to in this text as MODE I, comprises the chemical formation of atomic Cℓ with subsequent addition of HI. The second, or MODE II, involves the formation of CℓO radicals by a reduced initial addition of NO followed by a subsequent addition of NO and HI. The third kinetic mode of operation, MODE III, is a one-step addition procedure, in which the requisite chemistry and chemical laser pumping are performed *in situ* by a single addition of NO. Typical laser output powers of chemical MODES II and III were less than observed previously for MODE I (Ref. 8).

For the single-step addition (MODE III) experiments described here, the NO was in large excess of $C\ell O_2$ and HI. Under these conditions, the reaction sequence appears to be largely non-chain in character. It is believed that this is primarily due to the first reaction step:

$$NO + C\ell O_2 \rightarrow NO_2 + C\ell O$$

becoming more important relative to the chain-branching step $C\ell + C\ell O_2 \rightarrow 2C\ell O$. Experiments also suggest that the above initial reaction step involving NO may have an activation energy associated with it.

Modelling calculations indicate that the chain character of MODE III operation may be restored if <u>both</u> $C\ell O_2$ and NO are in excess of HI. Excess $C\ell O_2$ effectively compensates for the presence of HI, which removes Cℓ atoms and thereby acts as a load on the chain cycle.

Evidence has been found which indicates that the discrepancy in the output powers observed in the three modes of operation is at least partly due to the increased importance of HCℓ - NO V-V energy transfer in MODES II and III as compared to MODE I. This is a result of the high optimum NO concentrations found in MODES II and III operations.

It is believed that chemical laser efficiencies for operation in MODES II and III can be augmented if (a) the $C\ell O_2$ flow is in sufficient excess of HI to ensure efficient operation of the chain and, therefore, a rapid pumping rate of vibrationally excited $HC\ell$; and (b) the NO flow is not greater than the stoichiometric requirement of 2/1 in (a) in order to minimize V-V relaxation losses by $HC\ell^{\dagger}$ - NO collisions.

6.0 REFERENCES

1. Maylotte, D.H., Polanyi, J.C., and Woodall, K.B., "Energy Distribution Among Reaction Products·IV·X + HY (X≡Cℓ, Br; Y≡Br, I), Cℓ + DI", J. Chem. Phys., 57, 1547-1560 (1972).

2. Moore, C. Bradley, "An Electrically Pulsed HCℓ Laser", IEEE J. Quantum Electron. QE-4, 52 (1968).

3. Glaze, J.A., Finzi, J. and Krupke, W.F., "A Transverse Flow CW HCℓ Chemical Laser", Appl. Phys. Lett. 18, 173-175 (1971).

4. Naegeli, D.W., and Ultee, C.J., "A CW HCℓ Chemical Laser", Chem. Phys. Lett. 6, 121-122 (1970).

5. Linevsky, M.J. and Carabetta, R.A., Results presented at the 4th Conference on Chemical and Molecular Lasers, St. Louis, Mo., October 1974, Paper MB-7.

6. Bemand, P.P., Clyne, M.A.A. and Watson, R.T., "Reactions of Chlorine Oxide Radicals. Part 4. Rate Constants for the Reactions Cℓ + OCℓO, O + OCℓO, H + OCℓO, NO + OCℓO and O + CℓO", J.C.S. Faraday Trans. I, 69, 1356-1374 (1973).

7. Suart, R.D., Snelling, D.R., Foster, K.D. and Arnold, S.J., "Purely Chemical Laser Based on Chlorine Atom Reactions: Hybrid CO_2 Laser", DREV R-4015/76. UNCLASSIFIED.

   Suart, R.D., Snelling, D.R. and Arnold, S.J., "Purely Chemical Laser Based on Chlorine Atom Reactions: $C\ell O_2$ - NO Reaction as Chlorine Atom Source", DREV R-4014/76. UNCLASSIFIED.

8. Foster, K.D., Suart, R.D. and Snelling, D.R., "An Efficient, Purely Chemical HCℓ Laser", DREV R-4059/76. UNCLASSIFIED.

9. Woodward, E.R., Petroe, G.A. and Vincent, G.P., "A New Process for Producing Chlorine Dioxide for Industrial Use", Trans. Am. Inst. of Chem. Engineers 40, 271-290 (1944), (Pub. 1945).

10. Suart, R.D., Snelling, D.R., Foster, K.D. and Lambert, R., "Purely Chemical Laser Based on Chlorine Atom Reactions $C\ell O_2$ Generator", DREV R-4005/76. UNCLASSIFIED.

11. Arnold, S.J. and Blanchard, A., "Dolphin, A General Program for the Treatment of Chemical Rate Equations", DREV Report (to be published). UNCLASSIFIED.

12. Arnold, S.J., Snelling, D.R., Foster, K.D. and Suart, R.D., "Computer Simulation of the Chemistry of HCℓ Laser Systems", DREV Report (to be published). UNCLASSIFIED.

13. MacDonald, R.G., Moore, C. Bradley, Smith, I.W.M. and Wodarczyk, F.J.,"Vibrational Relaxation of HCℓ (v=1) by Cℓ Atoms", J. Chem. Phys., 62, 2934-2938 (1975).

14. Zittel, P.F. and Moore, C. Bradley, "V → T, R and V → V Relaxation in DCℓ System", J. Chem. Phys. 58, 2922-2928 (1973).

15. Clark, T.C., Clyne, M.A.A. and Stedman, D.H., "Mechanism of Formation of Triatomic Molecules in Atomic Combination Reactions. Part 1. Formation of CℓNO and CℓCO in Reactions of Atomic Chlorine", Trans. Faraday Soc. 62, 3354-3365 (1966).

APPENDIX A

A generalized computer model describing the chemical processes taking place in the laser has been developed. The mechanics of the computer simulation are described in detail in "DOLPHIN, A General Program for the Treatment of Chemical Rate Equations" (Ref. 11). It is sufficient to note that the time evolution of the reaction ensemble was simulated using a Runge-Kutta numerical integration routine.

This Appendix consists of a listing of the processes considered in a computer simulation of reacting mixtures typically used in practice during laser experiments. Table A-I lists those reactions used to produce chlorine atoms and Table A-II lists those used to generate vibrational excitation during the reaction of Cℓ atoms with HI and the subsequent V-V exchange reactions of the HCℓ thus formed. Additional possible V-V exchange reactions between HCℓ - HI are not considered due to the lack of rate data. Table A-III lists those V-T transfer reactions of HCℓ for which reliable rate data are available. No rate data are available for the V-T transfer of HCℓ with the species, NO_2, I_2, I, O_2, HI or NOCℓ all of which are present in appreciable concentrations at various ti[illegible] the evolution of the reacting mixture. Table A-IV gives additional reactions of iodine atoms.

A more detailed account of the modelling studies is given in Ref. 12 of text. This includes an appraisal of the relevant rate data.

The tables are printed directly by a line printer with the following notations being used: 1.0E-11 = 1.0×10^{-11} and Cℓ2=$Cℓ_2$ etc.

Reference notes for: Tables A-I to A-IV.

A. Rate constants calculated for 300 K; M= He

B. The overall rate constant for the reaction $2C\ell O \xrightarrow{k_f}$ products is given in Ref. A-3 as $(1.3 \pm 0.1) \times 10^{-12} \exp(-1150 \pm 50/T)$. Clyne et al (Ref. A-10) indicate that at 298 K reaction (4) accounts for 4.0% of the total reaction. The ratio of reaction (5) to reaction (6) is not accurately known. Watson (Ref. A-11) indicates that $k_5/k_6 \sim 1$ at low pressures (1 to 3 torr) while Clyne et al (Ref. A-10) state that reaction (5) is a major reaction channel in the second order decay of CℓO. For the present calculations, $k_4 = k_6 = 0$ and $k_5 = k_f$.

C. A value of the rate constant, k_7, was calculated from the relationships:

$$C\ell OO + M \underset{k_7}{\rightleftarrows} C\ell + O_2 + M$$

$$k_7 = \frac{k_{equil}}{k_8} = \frac{e^{-\Delta H/RT} e^{\Delta S/R}}{k_8}$$

where $k_8 = 5.6 \times 10^{-34}$ and the required thermodynamic data from Ref. A-12.

D. A value of the rate constant k_{10} was obtained from the ratio $k_9/k_{10} = 15$ of Ref. A-13 and the value of $k_9 = 1.56 \times 10^{-10}$ from Ref. A-5.

E. Basco and Dogra (Ref. A-14) in a study of CℓO recombination over a similar total pressure range to that of Johnson et al (Ref. A-5) found no dependence of the overall rate constant on M. For the present calculations $k_{11} = 0$.

F. The value of the rate constant k_{16} is assumed to be equal to that of k_{13}.

G. The value of the overall rate constant

$Cl + HI\ (v=0) \rightarrow HCl\ (v=n) + I \quad n=0,1,2,3,4$

is 1.64×10^{-10} (Ref. A-15). Anlauf et al (Ref. A-16) give the relative rates of formation of HCl into v=1,2,3,4 as 0.30:0.6:1.0:0.7. It was assumed that the rate of formation into v=0 was 1/3 of that into v=1.

H. The values of the rate constants for

$Cl + HI\ (v=1) \rightarrow HCl\ (v=n) + I \quad n=0,1,2,3,4$

are assumed to be the same as that of G.

I. The average value of the rate constants given in Ref. A-17-A-19 was used.

J. No reliable values of the rate constants for reactions (29) to (46) exist. Consequently k_i $(29 \leq i \leq 46)$ is set equal to zero for the present calculations. A detailed discussion of the V-V transfer processes occurring for HCl is given in Ref. A-20.

K. The values of the rate constants for reactions (50) to (54) were obtained from the ratios given in Ref. A-23, and the value of $k_{49} = 8.8 \times 10^{-12}$ is given in Ref. A-22.

L. The values of the rate constants for reactions (55) to (63) were obtained by interpolation from the data of Ref. A-23.

M. $k\ [HCl(v=n)] = nk\ [HCl(v=1)]$

N. The average value of the rate constants given in Ref. A-23-A-25 was used.

O. The value of the rate constant for the reaction

$I\ (^2P_{\frac{1}{2}}) + NOC\ell \rightarrow IC\ell + NO$

$k = 6.2 \times 10^{-12}$ given in Ref. A-28 is assumed to be the same as that for the comparable reaction with $I\ (^2P_{3/2})$.

P. Clyne et al (Ref. A-31) states that the heteroatom recombination

$I + C\ell + M \rightarrow IC\ell + M$

is noticeably faster than the homoatom recombination

$C\ell + C\ell + M \rightarrow C\ell_2 + M$

Consequently the value of the rate constant for reaction (12) was multiplied by 1.5 to give an approximate value for the rate constant 81.

TABLE A-I

	REACTION	RATE CONSTANT	REFERENCE
1	CL + OCLO → CLO + CLO	5.9 E-11	1
2	NO + OCLO → CLO + NO2	3.4 E-13	1
3	NO + CLO → CL + NO2	1.7 E-11	2
4	CLO + CLO → CL + OCLO		
5	CLO + CLO → CLOO + CL	2.6 E-14	3L
6	CLO + CLO → CL2 + O2		
7	CLOO + M → CL + O2 + M	1.34E-14	C
8	CL + O2 + M → CLOO + M	5.6 E-34	4
9	CL + CLOO → CL2 + O2	1.56E-10	5
10	CL + CLOO → CLO + CLO	1.04E-11	L
11	CLO + CLO + M → CL2 + O2 + M	6.6 E-32	5E
12	CL + CL + M → CL2 + M	6.39E-33	6
13	NOCL + CL → NO + CL2	3.0 E-11	7
14	NO + CL + M → NOCL + M	9.3 E-32	E
15	NO2 + CL + M → NO2CL + M	7.2 E-31	9
16	NO2CL + CL → NO2 + CL2	3.0 E-11	F

TABLE A-II

	REACTION	RATE CONSTANT	REFERENCE
17	CL + HI(V=0) → HCL(V=0) + I	6.07E-12	5
18	CL + HI(V=0) → HCL(V=1) + I	1.62E-11	5
19	CL + HI(V=0) → HCL(V=2) + I	3.64E-11	5
20	CL + HI(V=0) → HCL(V=3) + I	6.07E-11	5
21	CL + HI(V=0) → HCL(V=4) + I	4.25E-11	5
22	CL + HI(V=1) → HCL(V=0) + I	6.07E-12	H
23	CL + HI(V=1) → HCL(V=1) + I	1.82E-11	H
24	CL + HI(V=1) → HCL(V=2) + I	3.64E-11	H
25	CL + HI(V=1) → HCL(V=3) + I	6.07E-11	H
26	CL + HI(V=1) → HCL(V=4) + I	4.25E-11	H
27	HCL(V=1) + HCL(V=1) → HCL(V=2) + HCL(V=0)	4.09E-12	(17-19)I
28	HCL(V=2) + HCL(V=0) → HCL(V=1) + HCL(V=1)	2.85E-12	(17-19)I
29	HCL(V=2) + HCL(V=2) → HCL(V=3) + HCL(V=1)		J
30	HCL(V=3) + HCL(V=1) → HCL(V=2) + HCL(V=2)		J
31	HCL(V=3) + HCL(V=3) → HCL(V=4) + HCL(V=2)		J
32	HCL(V=4) + HCL(V=2) → HCL(V=3) + HCL(V=3)		J
33	HCL(V=4) + HCL(V=4) → HCL(V=5) + HCL(V=3)		J
34	HCL(V=5) + HCL(V=3) → HCL(V=4) + HCL(V=4)		J
35	HCL(V=2) + HCL(V=1) → HCL(V=3) + HCL(V=0)		J
36	HCL(V=3) + HCL(V=0) → HCL(V=2) + HCL(V=1)		J
37	HCL(V=3) + HCL(V=2) → HCL(V=4) + HCL(V=1)		J
38	HCL(V=4) + HCL(V=1) → HCL(V=3) + HCL(V=2)		J
39	HCL(V=4) + HCL(V=3) → HCL(V=5) + HCL(V=2)		J
40	HCL(V=5) + HCL(V=2) → HCL(V=4) + HCL(V=3)		J
41	HCL(V=3) + HCL(V=1) → HCL(V=4) + HCL(V=0)		J
42	HCL(V=4) + HCL(V=0) → HCL(V=3) + HCL(V=1)		J
43	HCL(V=4) + HCL(V=2) → HCL(V=5) + HCL(V=1)		J
44	HCL(V=5) + HCL(V=1) → HCL(V=4) + HCL(V=2)		J
45	HCL(V=4) + HCL(V=1) → HCL(V=5) + HCL(V=0)		J
46	HCL(V=5) + HCL(V=0) → HCL(V=4) + HCL(V=1)		J
47	HCL(V=1) + HI(V=0) → HCL(V=0) + HI(V=1)	1.66E-13	21
48	HCL(V=0) + HI(V=1) → HCL(V=1) + HI(V=0)	7.24E-15	21

TABLE A-III

	REACTION	RATE CONSTANT	REFERENCE
49	$HCL(V=1) + CL \rightarrow HCL(V=0) + CL$	2.6 E-12	22
50	$HCL(V=2) + CL \rightarrow HCL(V=1) + CL$	1.05E-12	23A
51	$HCL(V=2) + CL \rightarrow HCL(V=0) + CL$	4.11E-12	23A
52	$HCL(V=3) + CL \rightarrow HCL(V=2) + CL$	1.13E-11	23A
53	$HCL(V=3) + CL \rightarrow HCL(V=1) + CL$	5.66E-12	23A
54	$HCL(V=3) + CL \rightarrow HCL(V=0) + CL$	2.54E-12	23A
55	$HCL(V=4) + CL \rightarrow HCL(V=3) + CL$	1.47E-11	L
56	$HCL(V=4) + CL \rightarrow HCL(V=2) + CL$	7.63E-12	L
57	$HCL(V=4) + CL \rightarrow HCL(V=1) + CL$	3.67E-12	L
58	$HCL(V=4) + CL \rightarrow HCL(V=0) + CL$	3.37E-12	L
59	$HCL(V=5) + CL \rightarrow HCL(V=4) + CL$	1.19E-11	L
60	$HCL(V=5) + CL \rightarrow HCL(V=3) + CL$	9.89E-12	L
61	$HCL(V=5) + CL \rightarrow HCL(V=2) + CL$	5.25E-12	L
62	$HCL(V=5) + CL \rightarrow HCL(V=1) + CL$	4.64E-12	L
63	$HCL(V=5) + CL \rightarrow HCL(V=0) + CL$	4.3 E-12	L
64	$HCL(V=1) + NO \rightarrow HCL(V=0) + NO$	9.69E-14	24
65	$HCL(V=2) + NO \rightarrow HCL(V=1) + NO$	1.94E-13	M
66	$HCL(V=3) + NO \rightarrow HCL(V=2) + NO$	2.91E-13	M
67	$HCL(V=4) + NO \rightarrow HCL(V=3) + NO$	3.88E-13	M
68	$HCL(V=5) + NO \rightarrow HCL(V=4) + NO$	4.85E-13	M
69	$HCL(V=1) + HCL(V=0) \rightarrow HCL(V=0) + HCL(V=0)$	2.93E-14	(24-26)M
70	$HCL(V=2) + HCL(V=0) \rightarrow HCL(V=1) + HCL(V=0)$	5.85E-14	M
71	$HCL(V=3) + HCL(V=0) \rightarrow HCL(V=2) + HCL(V=0)$	8.78E-14	M
72	$HCL(V=4) + HCL(V=0) \rightarrow HCL(V=3) + HCL(V=0)$	1.17E-13	M
73	$HCL(V=5) + HCL(V=0) \rightarrow HCL(V=4) + HCL(V=0)$	1.46E-13	M
74	$HCL(V=1) + CL2 \rightarrow HCL(V=0) + CL2$	1.00E-14	27
75	$HCL(V=2) + CL2 \rightarrow HCL(V=1) + CL2$	2.00E-14	M
76	$HCL(V=3) + CL2 \rightarrow HCL(V=2) + CL2$	3.00E-14	M
77	$HCL(V=4) + CL2 \rightarrow HCL(V=3) + CL2$	4.00E-14	M
78	$HCL(V=5) + CL2 \rightarrow HCL(V=4) + CL2$	5.00E-14	M

TABLE A-IV

	REACTION	RATE CONSTANT	REFERENCE
79	$I + NOCL \rightarrow ICL + NO$	6.2 E-12	6
80	$CL + ICL \rightarrow CL2 + I$	6.0 E-12	29
81	$I + CL + M \rightarrow ICL + M$	1.0 E-32	E
82	$I + I + M \rightarrow I2 + M$	4.17E-33	30

REFERENCES

APPENDIX A

A-1 Bemand, P.P., Clyne, M.A.A. and Watson, R.T., "Reactions of Chlorine Oxide Radicals. Part 4. Rate Constants for the Reactions Cℓ + OCℓO, O + OCℓO, H + OCℓO, NO + OCℓO and O + CℓO", J.C.S. Faraday Trans. I. 69, 1356-1374 (1973).

A-2 Clyne, M.A.A. and Watson, R.T., "Kinetic Studies of Diatomic Free Radicals using Mass Spectrometry. Part 2. Rapid Bimolecular Reactions Involving the CℓO $X^2\Pi$ Radicals", J.C.S. Faraday Trans. I. 70, 2250-2259 (1974).

A-3 Clyne, M.A.A. and White, I.F., "Reactions of Chlorine Oxide Radicals. Part 3. Kinetics of the Decay Reaction of the CℓO ($X^2\Pi$) Radical", Trans. Faraday Soc. 67, 2068-2076 (1971).

A-4 Stedman, D.H., page 219 in Clyne, M.A.A. and Coxon, J.A., Proc. Roy. Soc. A303, 207-231 (1968).

A-5 Johnston, H.S., Morris, E.D. and Van den Bogaerde, J., "Molecular Modulation Kinetic Spectrometry. CℓOO and $C\ell O_2$ Radicals in the Photolysis of Chlorine in Oxygen", J. Am. Chem. Soc. 91, 7712-7727 (1969).

A-6 Widman, R.P. and DeGraff, B.A., "On the Gas-Phase Recombination of Chlorine Atoms", J. Phys. Chem. 77, 1325-1328 (1973).

A-7 Clyne, M.A.A. and Cruse, H.W., "Atomic Resonance Fluorescence Spectrometry for Rate Constants of Rapid Biomolecular Reactions. Part 1. Reactions O + NO_2, Cℓ + CℓNO, Br + CℓNO", J.C.S. Faraday Trans. II. 68, 1281-1299 (1972).

A-8 Clyne, M.A.A. and Stedman, D.H., "Recombination of Ground State Halogen Atoms. Part 2. Kinetics of the Overall Recombination of Chlorine Atoms", Trans. Faraday Soc. 64, 2698-2707 (1968).

A-9 Clyne, M.A.A. and White, I.F., unpublished data, see page 2882 of Clyne, M.A.A. and Cruse, H.W., Trans. Faraday Soc. 67, 2869-2885 (1971).

A-10 Clyne, M.A.A., McKenney, D.J. and Watson, R.T., "Reactions of Chlorine Oxide Radicals. Part 5. The Reaction $2C\ell O\ (X^2\Pi) \rightarrow$ Products", J.C.S. Faraday Trans. I. 71, 322-335 (1975).

A-11 Watson, R.T., "Chemical Kinetics Data Survey. VIII. Rate Constants of $C\ell O_x$ of Atmospheric Interest", NBSIR 74-516, page 28.

A-12 Wagman, D.D. and Garvin, D., "Provisional Thermochemical Data Sheets for $C\ell O$ and $C\ell OO$", Nat. Bur. Stand., Washington, D.C. (May 1974).

A-13 Nicholas, J.E. and Norrish, R.G.W., "Some Reactions in the Chlorine and Oxygen System Studied by Flash Photolysis", Proc. Roy. Soc. A307, 391-397 (1968).

A-14 Basco, N. and Dogra, S.K., "Reactions of Halogen Oxides Studied by Flash Photolysis", I. The Flash Photolysis of Chlorine Dioxide Proc. Roy. Soc. A323, 29-68 (1971).

A-15 Bergman, K. and Moore, C. Bradley, "Energy Dependence and Isotope Effect for the Total Reaction Rate of $C\ell$ + HI and $C\ell$ + HBr", J. Chem. Phys. 65, 643-649 (1975).

A-16 Anlauf, K.G., Maylotte, D.H., Pacey, P.D. and Polanyi, J.C., "Vibrational Population-Inversion and Stimulated Emission from the Continuous-Mixing of Chemical Reagents", Phys. Lett. 24A, 208-210 (1967).

A-17 Hopkins, B.M. and Chen, H.-L., "Vibrational Excitation and Relaxation of HCℓ (v=2) State", J. Chem. Phys. 57, 3816-3821 (1972).

A-18 Leone, S.R. and Moore, C. Bradley, "V→V Energy Transfer in HCℓ with Tunable Optical Parametric Oscillator Excitation", Chem. Phys. Lett. 19, 340-344 (1974).

A-19 Burak, I., Noter, Y., Ronn, A.M. and Szöke, A., "Vibration-Vibration Energy Transfer in Gaseous HCℓ", Chem. Phys. Lett. 17, 345-346 (1972).

A-20 Arnold, S.J., "V-V Energy Transfer Processes in HCℓ", DREV Report (to be published). UNCLASSIFIED.

A-21 Chen, H.-L. and Moore, C. Bradley, "Vibration-Vibration Energy Transfer in Hydrogen Chloride Mixtures", J. Chem. Phys. 54, 4080-4084 (1971).

A-22 MacDonald, R.G., Moore, C. Bradley, Smith, I.W.M. and Wodarczyk, F.J., "Vibrational Relaxation of HCℓ (v=1) by Cℓ Atoms", J. Chem. Phys. 62, 2934-2938 (1975).

A-23 Wilkins, R.L., "Vibrational Relaxation of HCℓ (v=1,2,3,6) by H and Cℓ Atoms", J. Chem. Phys. 63, 534-543 (1975).

A-24 Zittel, P.F. and Moore, C. Bradley, "V→T, R and V→V Relaxation in DCℓ Systems", J. Chem. Phys. 58, 2922-2928 (1973).

A-25 Chen, H.-L. and Moore, C. Bradley, "Vibration→Rotation Energy Transfer in Hydrogen Chloride", J. Chem. Phys. 54, 4072-4080 (1971).

A-26 Ahl, J.L. and Cool, T.A., "Vibrational Relaxation in the HF-HCℓ, HF-HBr, HF-HI, and HF-DF Systems", J. Chem. Phys. 58, 5540-5548 (1973).

A-27 Bott, J.F. and Cohen, N., "Vibrational Relaxation of HCℓ (v=1) in the Presence of Several Diatomic Molecules at 295-750°K", J. Chem. Phys. 63, 1518-1524 (1975).

A-28 Hathorn, F.G.M. and Husain, D., "Some Reactions of Electronically Excited Iodine Atoms, $I(5^2P_{\frac{1}{2}})$, with Halides and Oxides", Trans. Faraday Soc. 65, 2678-2684 (1969).

A-29 Clyne, M.A.A. and Cruse, H.W., "Atomic Resonance Fluorescence Spectrometry for the Rate Constants of Rapid Biomolecular Reactions. Part 2. Reactions Cℓ + BrCℓ, Cℓ + Br_2, Cℓ + ICℓ, Br + IBr, Br + ICℓ", J.C.S. Faraday Trans. II. 68, 1377-1387 (1972).

A-30 Chang, S.K., Clarke, A.G. and Burns, G., "Recombination of Br Atoms by Flash Photolysis Over a Wide Temperature Range. III. Br_2 in Xe, CF_4, SF_6", J. Chem. Phys. 54, 1835-1837 (1971).

A-31 Clyne, M.A.A. and Coxon, J.A., "The Formation and Detection of Some Low-lying Excited Electronic States of BrCℓ and other Halogens", Proc. Roy. Soc. A298, 424-452 (1967).

DREV REPORT 4060/77 (UNCLASSIFIED)

Bureau - Recherche et Développement, Ministère de la Défense nationale, Canada. CRDV, C.P. 880, Courcelette, Qué. GOA 1RO.

"Optimization of the Pre-Pumping $NO/C\ell O_2$ Chemistry in a Purely Chemical $HC\ell$ Laser"
by K.D. Foster, D.R. Snelling, R.D. Suart and S.J. Arnold

L'émission laser à 3.8 μm, provenant d'un laser au $HC\ell$ purement chimique, a été utilisée pour recueillir des renseignements sur la chimie du prépompage par le système $NO/C\ell O_2$. La réaction entre les atomes de chlore produits chimiquement et l'iodure d'hydrogène fournit le mécanisme de pompage. Le laser a fonctionné efficacement selon trois différents modes cinétiques ou chimiques. Ces modes se différencient par la façon dont le chlore est introduit dans la cavité laser, soit directement sous forme d'atomes de chlore, de radicaux $C\ell O$ ou de molécules de $C\ell O_2$. La comparaison des résultats expérimentaux de ces deux derniers modes avec ceux d'une simulation par ordinateur sur la disparition du $HC\ell$ permet d'expliquer les caractéristiques principales des relations entre la réaction de pompage et la chimie du prépompage.

DREV REPORT 4060/77 (UNCLASSIFIED)

Bureau - Recherche et Développement, Ministère de la Défense nationale, Canada. CRDV, C.P. 880, Courcelette, Qué. GOA 1RO.

"Optimization of the Pre-Pumping $NO/C\ell O_2$ Chemistry in a Purely Chemical $HC\ell$ Laser"
by K.D. Foster, D.R. Snelling, R.D. Suart and S.J. Arnold

L'émission laser à 3.8 μm, provenant d'un laser au $HC\ell$ purement chimique, a été utilisée pour recueillir des renseignements sur la chimie du prépompage par le système $NO/C\ell O_2$. La réaction entre les atomes de chlore produits chimiquement et l'iodure d'hydrogène fournit le mécanisme de pompage. Le laser a fonctionné efficacement selon trois différents modes cinétiques ou chimiques. Ces modes se différencient par la façon dont le chlore est introduit dans la cavité laser, soit directement sous forme d'atomes de chlore, de radicaux $C\ell O$ ou de molécules de $C\ell O_2$. La comparaison des résultats expérimentaux de ces deux derniers modes avec ceux d'une simulation par ordinateur sur la disparition du $HC\ell$ permet d'expliquer les caractéristiques principales des relations entre la réaction de pompage et la chimie du prépompage.

DREV REPORT 4060/77 (UNCLASSIFIED)

Bureau - Recherche et Développement, Ministère de la Défense nationale, Canada. CRDV, C.P. 880, Courcelette, Qué. GOA 1RO.

"Optimization of the Pre-Pumping $NO/C\ell O_2$ Chemistry in a Purely Chemical $HC\ell$ Laser"
by K.D. Foster, D.R. Snelling, R.D. Suart and S.J. Arnold

L'émission laser à 3.8 μm, provenant d'un laser au $HC\ell$ purement chimique, a été utilisée pour recueillir des renseignements sur la chimie du prépompage par le système $NO/C\ell O_2$. La réaction entre les atomes de chlore produits chimiquement et l'iodure d'hydrogène fournit le mécanisme de pompage. Le laser a fonctionné efficacement selon trois différents modes cinétiques ou chimiques. Ces modes se différencient par la façon dont le chlore est introduit dans la cavité laser, soit directement sous forme d'atomes de chlore, de radicaux $C\ell O$ ou de molécules de $C\ell O_2$. La comparaison des résultats expérimentaux de ces deux derniers modes avec ceux d'une simulation par ordinateur sur la disparition du $HC\ell$ permet d'expliquer les caractéristiques principales des relations entre la réaction de pompage et la chimie du prépompage.

DREV REPORT 4060/77 (UNCLASSIFIED)

Bureau - Recherche et Développement, Ministère de la Défense nationale, Canada. CRDV, C.P. 880, Courcelette, Qué. GOA 1RO.

"Optimization of the Pre-Pumping $NO/C\ell O_2$ Chemistry in a Purely Chemical $HC\ell$ Laser"
by K.D. Foster, D.R. Snelling, R.D. Suart and S.J. Arnold

L'émission laser à 3.8 μm, provenant d'un laser au $HC\ell$ purement chimique, a été utilisée pour recueillir des renseignements sur la chimie du prépompage par le système $NO/C\ell O_2$. La réaction entre les atomes de chlore produits chimiquement et l'iodure d'hydrogène fournit le mécanisme de pompage. Le laser a fonctionné efficacement selon trois différents modes cinétiques ou chimiques. Ces modes se différencient par la façon dont le chlore est introduit dans la cavité laser, soit directement sous forme d'atomes de chlore, de radicaux $C\ell O$ ou de molécules de $C\ell O_2$. La comparaison des résultats expérimentaux de ces deux derniers modes avec ceux d'une simulation par ordinateur sur la disparition du $HC\ell$ permet d'expliquer les caractéristiques principales des relations entre la réaction de pompage et la chimie du prépompage.